Energy 58 (2013) 448–457

Contents lists available at SciVerse ScienceDirect

Energy

journal homepage: www.elsevier.com/locate/energy

Energy and exergy analyses of a bottoming Rankine cycle for engine exhaust heat recovery

Sipeng Zhu [a], Kangyao Deng [a,*], Shuan Qu [b]

[a] Key Laboratory for Power Machinery and Engineering of Ministry of Education, Shanghai Jiao Tong University, Shanghai City 200240, China
[b] China North Engine Research Institute, Datong 037036, China

ARTICLE INFO

Article history:
Received 30 January 2013
Received in revised form
7 June 2013
Accepted 8 June 2013
Available online 13 July 2013

Keywords:
Rankine cycle
Engine
Waste heat recovery
Working fluid property
Evaporating pressure

ABSTRACT

In this paper, a theoretical study on the thermodynamic processes of a bottoming Rankine cycle for engine waste heat recovery is conducted from the viewpoints of energy balance and exergy balance. A theoretical formula and an exergy distribution map for qualitative analyses of the main operating parameters are presented under simplified conditions when exhaust gas is selected as the only heat source. Five typical working fluids, which are always selected by manufacturers for different types of engines, are compared under various operating conditions in Matlab software. The results show that working fluid properties, evaporating pressure and superheating temperature are the main factors influencing the system design and performances. The global recovery efficiency does not exceed 0.14 under typical operating conditions. Ethanol and R113 show better thermodynamic performances in the whole exhaust gas temperature range. In addition, the optimal evaporating pressure usually does not exist in engine exhaust heat recovery, and the distributions of exergy destruction are varied with working fluid categories and system design constraints.

1. Introduction

With the crude oil price increasing and the environment problems caused by greenhouse gases becoming more and more serious, the internal combustion engine (ICE) development appears to be challenged, which makes waste heat recovery (WHR) become a hot research subject. For current ICEs, the proportion of fuel energy converted into effective work at medium and high loads is about 30%～45% for the diesel engine or 20%～30% for the gasoline engine, and the rest is mainly brought into the environment by the exhaust gas and cooling system. There are three typical approaches of recovering ICE waste heat including thermoelectric generation, electrical or mechanical turbo compounding and steam or organic Rankine cycles [1]. The Rankine cycle, as a mature technique, has been widely used in low-grade WHR such as solar thermal, geothermal and vast amounts of industrial waste heat [2]. Also the Rankine cycle shows great potentials and has become the main research direction of engine WHR due to its high recovery efficiency.

Researches on Rankine cycles for engine WHR have made great progress since 1970 when the first energy crisis broke out. Selecting water and ethanol as working fluids, BMW conducted a two-loop Rankine cycle system on a four-cylinder gasoline engine to recover waste heat from the exhaust gas and the cooling system, and test bench measurements showed that an additional power of about 10% can be produced at typical highway cruising speeds [3]. Honda installed a steam Rankine cycle system in a hybrid vehicle to verify the WHR efficiency, and results of vehicle testing showed that the thermal efficiency is increased from 28.9% to 32.7% at 100 km/h constant vehicle speed [4]. Cummins proposed an improvement of 10% fuel efficiency in class 8 trucks through an organic Rankine cycle (ORC) together with other measures. In those studies, R245fa was selected as the working fluid, and the ORC was driven by waste heat of the exhaust gas recirculation (EGR) coolant and exhaust gas [5]. Thomas et al. [6] equipped an ORC system on a 1.9 L light duty diesel engine and conducted experimental researches in Oak Ridge National Laboratory. The outcomes indicated that the peak brake thermal efficiency can be improved from 42.6% to 45%, which demonstrated that even a light-duty diesel engine can benefit from the installation of an ORC system. Zhang et al. [7] established a simplified experimental system to recovery the exhaust heat from a gasoline engine with R113 as the working fluid and testified a practical efficiency about 14.4% of the Rankine cycle

Abbreviations: WHR, waste heat recovery; ICE, internal combustion engine; ORC, organic Rankine cycle; EGR, exhaust gas recirculation.

* Corresponding author. Tel./fax: +86 021 34206380.
E-mail addresses: sipengzhu@126.com (S. Zhu), kydeng@sjtu.edu.cn (K. Deng).

0360-5442/$ – see front matter © 2013 Elsevier Ltd. All rights reserved.
http://dx.doi.org/10.1016/j.energy.2013.06.031

Nomenclature

c_p	specific heat capacity [kJ/kg K]
$\dot{H}$	enthalpy flow [kW]
$\dot{I}$	exergy destruction rate [kW]
h	specific enthalpy [kJ/kg]
ln	natural logarithm
$\dot{m}$	mass flow rate [kg/s]
P	pressure [bar]
$\dot{Q}$	heat flow [kW]
R	Rankine cycle
R_g	ideal gas constant [kJ/kg K]
S	entropy [kJ/K]
s	specific entropy [kJ/kg K]
T	temperature [K]
ΔT	temperature difference [K]
$\dot{W}$	power [kW]

Greek symbols

π	pressure ratio [−]
γ	latent heat of fluid [kJ/kg]
η	efficiency [%]

Subscripts

cond	condenser
cr	critical
exh	exhaust gas
eva	evaporation
l	liquid phase
max	maximal
min	minimal
p	pump
sup	superheat
t	turbine
tot	total
wf	working fluid
0	reference state

a-d, 1-5, 1′-5′ state points in waste heat recovery system

system. Park et al. [8] selected ethanol as the working fluid and designed compact system components applied on a 10.8-L heavy duty truck diesel engine. All those references indicated that the cost, weight and size of the Rankine cycle components should be considered seriously for vehicle applications.

Also, many numerical analyses of the bottoming Rankine cycle system were carried out with thermodynamic models. Serrano et al. [9] studied different kinds of heat sources and system configurations on a heavy duty diesel engine from viewpoints of the external irreversibility and technological complexity. Vaja and Gambarotta [10] conducted parametric analyses to determine the optimal evaporating pressures of three different kinds of working fluids and compared the global system efficiencies of three different cycle configurations. Wang et al. [11] investigated nine different organic working fluids when net power output were fixed at 10 kW, and the optimal control principles of the ORC system under transient processes were also discussed. Katsanos et al. [12] indicated that it was necessary to modify Rankine cycle parameters due to the variation of the exhaust gas temperature with engine load. Arias et al. [13] compared three different configurations of the Rankine cycle system in a hybrid vehicle. Srinivasan et al. [14] quantified potential improvements in fuel conversion efficiency and specific emissions with hot EGR and ORC. Chammas and Clodic [15] claimed that the potential of the Rankine cycle for improving the net fuel consumption on hybrid vehicles can be as high as 32% with organic working fluids. Shu et al. [16] analyzed the combined thermoelectric generator and ORC in exhaust heat recovery of the ICE theoretically. Yu et al. [17] conducted simulations and thermodynamic studies on an ORC system to recover waste heat both from engine exhaust gas and jacket water with R245fa as the working fluid. Tian et al. [18] screened 20 working fluids and conducted techno-economical analyses for an ORC system on the rated condition of one popular commercial diesel generator set.

For different types of ICEs, the waste heat distributions are varied, the exhaust gas temperatures are at different levels, and the design constraints of system components are also varied for different vehicle applications. All those factors make the Rankine cycle systems for engine WHR varied in many aspects such as the working fluid selection, the system configuration and the operating parameters in the temperature-entropy diagram. Although many experimental and numerical researches on the Rankine cycle have been reported in recent years, most of them focused on only one type of the ICE [3,4,6,8,12,13,17] or a fixed heat source temperature [7,10,11,16,18] as mentioned above, and almost no comparison of Rankine cycle systems for different ICEs was presented. Also few detailed theoretical analyses of the Rankine cycle for engine WHR was published due to the fast development of convenient simulation tools. In order to figure out effects of the main operating parameters on the system performance precisely and provide a foundational understanding of the energy and exergy transfer processes, the basic theoretical analyses based on energy balance and exergy balance, which show us straightforward conclusions, are necessary to be conducted.

In this study, a theoretical formula was first proposed under simplified conditions to analyze the main operating parameters of the Rankine cycle qualitatively, and an exergy distribution map was drawn to explain the exergy destruction processes. Simulation models were built in Matlab software to investigate the influences of those parameters which could not be concluded from theoretical analyses. With system design constraints, five typical working fluids including water, ethanol, R113, R123 and R245fa, which are always selected for different types of ICEs, were compared under different heat source conditions and evaporating pressures. Exergy destruction of system components was also studied with different working fluids and operating parameters.

2. Thermodynamic models of Rankine cycle

For ICEs, the amount of waste heat in exhaust gas and cooling water occupies more than half of the total fuel energy, and the proportions of energy in those two waste heat sources are at the same level and vary with engine operating conditions. In general, the exhaust gas temperature at full load ranges from 400 to 600 °C for the diesel engine or 600–900 °C for the gasoline engine, which is much higher than that of cooling water. According to the temperature levels of waste heat sources, working fluids of Rankine cycles are always preheated by the cooling water and superheated by the exhaust gas. For some diesel engines, there may be intercooler or ERG cooler waste heat, which makes the configurations of Rankine cycles varied and complicated if more waste heat is expected to be recovered. In order to simplify the system construction, only the exhaust gas is considered as the heat source in the following sections.

2.1. System description

Fig. 1 shows the schematic view of the Rankine cycle system. The whole recovery system consists of the following processes: the working fluid pumping process 3-4, evaporating process 4-1, expanding process 1-2, and condensing process 2-3; the heat release process of exhaust gas a-b; the heat absorption process of cooling water d-e.

Organic working fluids with lower critical temperatures are always selected for the low-grade waste heat source whose temperature is normally lower than 230 °C, and superheating is not considered from the thermodynamic viewpoint. In contrast, engine exhaust gas can be regarded as a medium or high-grade waste heat source, and compactness is an essential issue in the Rankine cycle system for vehicle applications. Working fluids always need to be superheated considering the vehicle operation [4,6,19], which make the *T–s* diagram different from that of the traditional low-grade Rankine cycle system. For engine WHR, superheating cannot only insure the dryness of wet fluids after expanding but also reduce the needed mass flow rates of dry fluids, which can in return reduce the size and cost of every system component. Also control strategies should be adopted at low loads since the low-temperature exhaust gas might not be sufficient to superheat the working fluid.

Fig. 2 illustrates the thermodynamic processes of the bottoming Rankine cycle system on the *T–s* diagram. Processes 3-4s and 1-2s are the isentropic pumping process and isentropic expanding process, respectively. State points 5 and 5′ of the working fluid represent the saturated liquid and saturated vapor in the evaporator, respectively. Compared with expanding and pumping processes, pressure drops in the evaporator and condenser can be neglected [10]. The heat destruction between every system component and the environment can also be ignored in the following analyses [18].

For a steady heat source condition, the global recovery efficiency η_{tot}, which indicates the proportion of the expander output power to the exhaust gas energy, can be expressed as

$$\eta_{tot} = \eta_{exh}\eta_R \tag{1}$$

where η_{exh} and η_R are the exhaust gas utilization efficiency and the Rankine cycle efficiency, respectively, and can be calculated by

$$\eta_{exh} = \frac{h_a - h_c}{h_a - h_0} \tag{2}$$

$$\eta_R = \frac{h_1 - h_2 - (h_4 - h_3)}{h_1 - h_4} \tag{3}$$

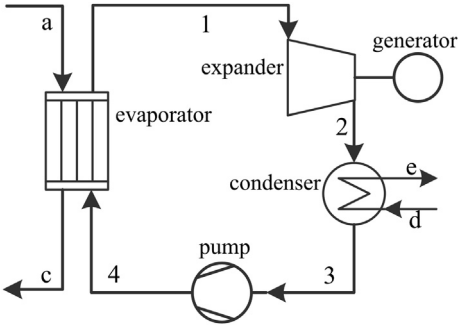

Fig. 1. Schematic view of the WHR system.

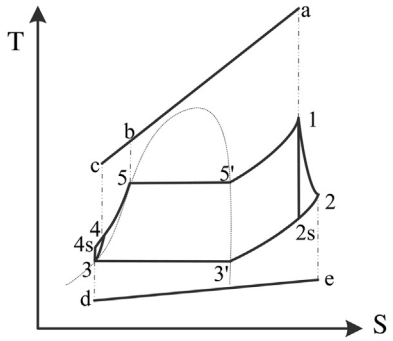

Fig. 2. *T–s* diagram of the bottoming Rankine cycle.

where subscript 0 indicates the environment condition, and other subscripts are described in Fig. 2.

2.2. Theoretical formula of the global recovery efficiency

2.2.1. Minimum temperature difference of the evaporator

The minimum temperature difference (MTD) is an important design parameter of the evaporator, and the pinch point analysis has been widely used in low-grade waste heat recovery [20,21]. The cost of unit WHR decreases with the increase of the MTD, while the exergy destruction of the evaporator increases at the same time. So it's better to choose a reasonable value for the MTD from the cost-effective view. Fig. 3 shows the temperature curves in the cold and hot sides of the evaporator. It can be concluded that the MTD can only occur at the inlet and outlet of the evaporator and the pinch point of the evaporating process. Considering the constraints of the evaporator design and the maximum thermal steady temperature of the working fluid, the MTD usually does not occur at the inlet point of the exhaust gas.

So the place where the MTD occurs mainly depends on the gradients of temperature curves in the preheating process. For working fluids in the evaporator, the relationship between the temperature and the heat transfer flux can be described as Eq. (4), and the criterion that the MTD occurs at the pinch point of the evaporating process can be deduced and given as Eq. (5).

$$d\dot{Q} = \dot{m}c_p dT \tag{4}$$

$$\left(\dot{m}_{exh}/\dot{m}_{wf}\right) > \left(c_{p,l}/c_{p,exh}\right) \tag{5}$$

where $\dot{m}_{exh}$ and $\dot{m}_{wf}$ are the mass flow rates of the exhaust gas and the working fluid, respectively, $c_{p,exh}$ and $c_{p,l}$ are the average

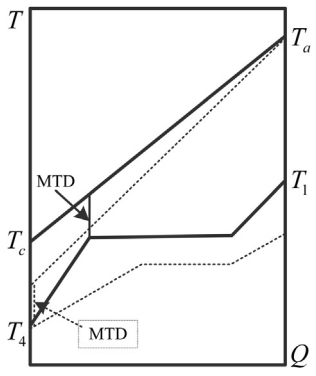

Fig. 3. *T–Q* diagram of the evaporator.

isobaric heat capacity of the exhaust gas and the working fluid in the corresponding temperature range, respectively. According to Eq. (5), the MTD will occur at the pinch point of the evaporating process when the working fluid has a lower mass flow rate and smaller average isobaric heat capacity in the liquid state, and vice verse.

2.2.2. Global recovery efficiency

In order to deduce the theoretical formula of the global recovery efficiency, some hypotheses are presented as follows: the MTD occurs at the pinch point of the evaporating process; the viscous friction of the working fluid in pipes is ignored; the isobaric heat capacity of the exhaust gas is assumed to be constant; the pumping power is neglected relative to the expander output power. Combined with Fig. 2, the theoretical formula of the global recovery efficiency can be deduced as follows.

From the heat transfer process of the evaporator, Eq. (6) can be drawn as

$$\frac{h_a - h_c}{h_1 - h_4} = \frac{h_a - h_b}{h_1 - h_5} \tag{6}$$

Substituting Eqs. (2), (3) and (6) into (1), the global recovery efficiency can be described as

$$\begin{aligned}\eta_{\text{tot}} &= \tfrac{h_a-h_b}{h_a-h_0}\tfrac{h_1-h_2}{h_1-h_5} = \tfrac{h_a-h_b}{h_a-h_0}\tfrac{\eta_t(h_1-h_{2s})}{h_1-h_5} \\ &= \tfrac{T_a-(T_5+\Delta T_{\min})}{T_a-T_0}\eta_t\tfrac{(h_1-h_3)-(h_{2s}-h_3)}{h_1-h_5}\end{aligned} \tag{7}$$

where $\Delta T_{\min}$ is the MTD in the evaporator, η_t is the isentropic efficiency of the expander, which is defined as the ratio between the actual expansion power and the isentropic expansion power.

The thermodynamic expression of specific entropy can be described as

$$\mathrm{d}s = \frac{c_p}{T}\mathrm{d}T - \left(\frac{\partial v}{\partial T}\right)_p \mathrm{d}P \tag{8}$$

Regardless of the pressure drop in the evaporator, the specific entropy changes of the heat absorption processes can be expressed as

$$s_5 - s_3 \approx c_{p,l} \ln \frac{T_5}{T_3} \tag{9}$$

$$s_{5'} - s_5 = \frac{\gamma}{T_5} \tag{10}$$

$$s_1 - s_{5'} \approx c_{p,\text{sup}} \ln \frac{T_5 + \Delta T_{\text{sup}}}{T_5} \tag{11}$$

where $c_{p,\text{sup}}$ and $c_{p,l}$ are the average isobaric heat capacity of the gas and liquid state of the working fluid in the corresponding temperature range, respectively, γ is the latent heat at the evaporating temperature, and ΔT_{sup} is the superheating temperature difference between state point 1 and point 5′.

The gradients of isobaric lines of the superheated vapor in the T–s diagram can be calculated as

$$\frac{\mathrm{d}T}{\mathrm{d}s} = \frac{T}{c_p} \tag{12}$$

In order to simplify the thermodynamic processes located on the right side of the saturated vapor line in the T–s diagram, here we assumed that the high temperature superheated vapor can be treated as the ideal gas, which will bring errors for the final derivative formula. For the ideal gas, the gradients of isobaric lines of the superheated vapor in the T–s diagram only depend on the temperature. If the temperature difference between line 5′1 and line 3′2 is not too large, we can assume that line 5′1 and line 3′2 are parallel in the T–s diagram. The changes of specific enthalpy of the working fluid can be further expressed as Eqs. (13) and (14).

$$h_1 - h_5 \approx \gamma + c_{p,\text{sup}}\Delta T_{\text{sup}} \tag{13}$$

$$(h_1 - h_3) - (h_{2s} - h_3) \approx \frac{1}{2}(T_5 - T_3)[(s_1 - s_5) + (s_1 - s_3)] \tag{14}$$

Substituting Eqs. (9)–(11), (13), (14) into (7), the final expression of the global recovery efficiency can be described as

$$\eta_{\text{tot}} = \frac{T_a - (T_5 + \Delta T_{\min})}{T_a - T_0}\eta_t \frac{(T_5 - T_3)\left[c_{p,\text{sup}} \ln \frac{T_5+\Delta T_{\text{sup}}}{T_5} + \frac{\gamma}{T_5} + \frac{1}{2}c_{p,l} \ln \frac{T_5}{T_3}\right]}{\gamma + c_{p,\text{sup}}\Delta T_{\text{sup}}} \tag{15}$$

If the MTD occurs at the inlet point of the working fluid, the exhaust gas temperature out of the evaporator can be directly calculated with the condensing temperature, and the global recovery efficiency can be deduced as Eq. (16) in the same way as above.

$$\eta_{\text{tot}} = \frac{T_a - (T_3 + \Delta T_{\min})}{T_a - T_0}\eta_t \frac{(T_5 - T_3)\left[c_{p,\text{sup}} \ln \frac{T_5+\Delta T_{\text{sup}}}{T_5} + \frac{\gamma}{T_5} + \frac{1}{2}c_{p,l} \ln \frac{T_5}{T_3}\right]}{c_{p,l}(T_5 - T_3) + \gamma + c_{p,\text{sup}}\Delta T_{\text{sup}}} \tag{16}$$

Since the high pressure superheated vapor cannot be considered as the ideal gas in a real condition, the isobaric lines in the T–s diagram may not be exactly parallel. Also the saturated vapor line may not be approximately vertical with the entropy axis for different working fluids. Those assumptions may bring relatively large errors but still can be used for a qualitative investigation. If the correlative expression of latent heat of the working fluid is given as in Ref. [22], more detailed formulae can be obtained for theoretical analyses.

After confirming the place where the MTD occurs with Eq. (5), the influences of all the primary parameters on the Rankine cycle performance can be obtained with Eq. (15) or (16), which provides an effective way for parameter selections and system optimizations. From the theoretical formulae, conclusions can be drawn as follows: the global recovery efficiency increases with the decrease of the MTD and the condensing temperature; with the increase of the exhaust gas temperature, the global recovery efficiency increases due to the high exergy fraction; since values of the latent heat and the isobaric heat capacity of the working fluid are determined by the evaporating temperature and the superheating temperature, effects of those two temperatures on the global recovery efficiency rely on the working fluid selection and cannot be learned from the deduced formulae directly; there may exist an optimal evaporating temperature or pressure since the first part and the last part in Eq. (15) change adversely with the increase of the evaporating temperature.

2.3. Analysis of exergy distributions

Since the traditional first law theory often fails to provide a better insight into thermodynamic processes, the availability or exergy analysis has been widely used to study the ICE operation [23]. For ICEs, the majority of the fuel availability is distributed between the indicated work , the availability destroyed in the combustion process, the availability moved to the cylinder walls via heat transfer and the availability leaving the cylinder with the exhaust gas.

To deduce the large portion of exergy destruction during the combustion process, alternative fuels have been widely researched [24–26]. Rakopoulos and Kyritsis [24] compared methane, methanol and dodecane fuels on a direct-injection diesel engine and reached a fundamental conclusion that the decomposition of lighter fuels leads to less entropy generation compared to heavier fuels, which is verified to decrease the combustion irreversibility. Rakopoulos et al. [25] continued to study the mechanism of entropy generation in the combustion process with mixtures of hydrogen and natural gas. Results indicated that the combustion irreversibility decreases with the increase of hydrogen content due to the particular characteristic of hydrogen combustion. Also another way to improve the exergy efficiency of the ICE is to explore the availability from the exergy losses in the exhaust gas and cooling water. Due to the high temperature of the exhaust gas, the availability in the exhaust gas can be more easily recovered.

In availability analyses of thermal systems, the availability can be customarily divided into two parts [27]: the thermomechanical availability which refers to the maximum useful mechanical work that can be extracted as the system comes into thermal and mechanical equilibrium with the surrounding atmosphere, and the chemical availability which consists of the diffusion availability and the reactive availability [26]. Since most researchers have not taken into account the term of chemical availability in their analyses due to the practical difficulty in exploiting this portion of availability [23], only the thermomechanical availability of the exhaust gas is considered in the following exergy analysis of the bottoming Rankine cycle system.

2.3.1. Exergy destruction of finite heat capacity

According to Carnot's theorem, the maximum possible efficiency η_{car} can be described as Eq. (17) when the exhaust gas temperature and the environment temperature are fixed at T_a and T_0, respectively.

$$\eta_{car} = 1 - T_0/T_a \tag{17}$$

Since the isobaric heat capacity of the exhaust gas is finite, the heat source temperature drops when it flows through the evaporator, which makes the actual maximum efficiency lower than that of the Carnot cycle. Without considering the pressure drop of the exhaust gas and assuming the isobaric heat capacity to be constant, the actual maximum efficiency η_{max} that can be achieved is calculated as

$$\eta_{max} = \frac{\int_{T_0}^{T_a} c_p\left(1-\frac{T_0}{T}\right)\mathrm{d}T}{\int_{T_0}^{T_a} c_p \mathrm{d}T} = 1 - \frac{T_0}{T_a - T_0}\ln\frac{T_a}{T_0} \tag{18}$$

Compared with the output power of the Carnot cycle with the same heat source temperature, the maximum useful power of the exhaust gas is relatively lower, and the virtual exergy destruction rate $\dot{I}_{exh}$ caused by the finite heat capacity of the exhaust gas in the real heat transfer process is calculated by

$$\dot{I}_{exh} = \dot{Q}\left(\frac{T_0}{T_a - T_0}\ln\frac{T_a}{T_0} - \frac{T_0}{T_a}\right) \tag{19}$$

2.3.2. Exergy destruction in heat transfer and power processes

In the Rankine cycle WHR system, there are irreversibility destruction in every system component caused by heat transfer processes or nonisentropic power processes. The exergy destruction rate of the evaporator can be divided into two parts: the internal exergy destruction rate $\dot{I}_{41}$ caused by the temperature difference between cold and hot sides of the evaporator and the external exergy destruction rate $\dot{I}_{c0}$ which flows into the environment. The exergy destruction rates of the expander $\dot{I}_{12}$ and the pump $\dot{I}_{34}$ are caused by the nonisentropic expanding and pumping processes, respectively. The exergy destruction rate $\dot{I}_{cond}$ in the condenser can also be divided into two parts: the internal exergy destruction rate $\dot{I}_{23}$ and the external exergy destruction rate $\dot{I}_{de}$.

Assuming the Rankine cycle system reaches a steady state, the exergy destruction rate of every control volume can be expressed as

$$\dot{I} = T_0\frac{\mathrm{d}S_g}{\mathrm{d}t} = \dot{m}T_0\left[\sum_{out} s - \sum_{in} s - \sum_k \frac{q_k}{T_k}\right] \tag{20}$$

where T_0 is the environmental temperature, T_k is the temperature of each heat source, q_k is the heat transferred from each heat source to the control volume. All those exergy destruction rates can be calculated with Eqs. (21)–(25), respectively.

$$\dot{I}_{41} = T_0\left[\dot{m}_{wf}(s_1 - s_4) + \dot{m}_{exh}(s_c - s_a)\right] \tag{21}$$

$$\dot{I}_{c0} = \dot{m}_{exh}T_0\left[(s_0 - s_c) + \frac{(h_c - h_0)}{T_0}\right] \tag{22}$$

$$\dot{I}_{12} = \dot{m}_{wf}T_0(s_2 - s_1) \tag{23}$$

$$\dot{I}_{34} = \dot{m}_{wf}T_0(s_4 - s_3) \tag{24}$$

$$\dot{I}_{cond} = \dot{I}_{23} + \dot{I}_{de} = \dot{m}_{wf}T_0\left[(s_3 - s_2) + \frac{h_2 - h_3}{T_0}\right] \tag{25}$$

2.3.3. Exergy flow map

Zhu [28] adopted a $(1 - T_0/T) - \dot{H}$ diagram to analyze a dual cycle system and effects of parameters on the exergy efficiency, which explained the exergy destruction of system components clearly. Compared with the other exergy transfer processes, the exergy destruction rate in the pumping process can be neglected [20]. With the exergy analyses of the Rankine cycle for exhaust gas WHR, the distributions of exergy destruction can be drawn.

As shown in Fig. 4, the area above the heat releasing curve "abc0" indicates the virtual exergy destruction rate caused by finite heat capacity of the exhaust gas; the area of "abc0ga" represents the maximum useful power which can be achieved from the exhaust gas; the areas of "abc355'1a" and "c0dc" are the internal and external exergy destruction rates of the evaporator, respectively; the areas of "23′3de2" and "edfe" represent the internal and external exergy destruction rates of the condenser, respectively; obviously, the remaining area of "15′533′2fg1" in the map indicates the sum of the output power and the exergy destruction rate of the expander.

Also the abscissa shows the energy transfer processes: line "0-g" indicates the amount of energy in the exhaust gas; line "d-g" represents the amount of heat transferred in the evaporator; line "d-f" indicates the amount of heat released in the condenser; line "f-g" represents the expander output power. The exhaust gas utilization efficiency and the Rankine cycle efficiency can also be expressed with those lines.

With the above exergy and energy analyses, effects of primary operating parameters on the exergy destruction of system components can be indicated by the variation of the curves and points in Fig. 4. Note that just one parameter is changed for one time, and

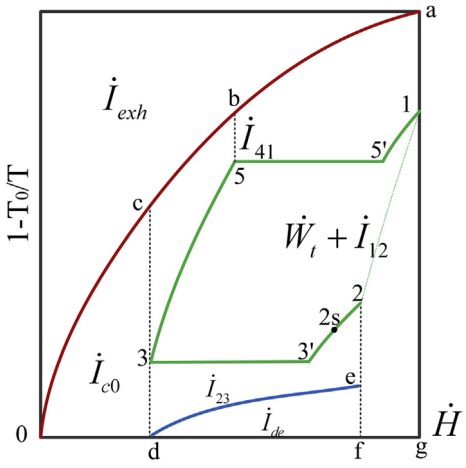

Fig. 4. Distributions of exergy destruction.

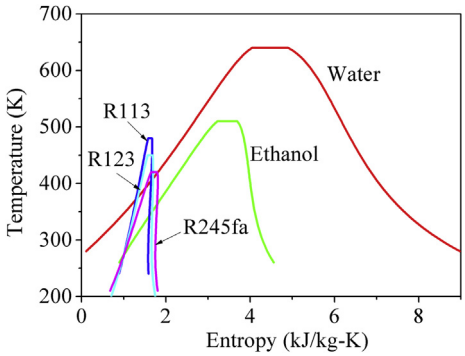

Fig. 5. *T–s* plots of working fluids.

main conclusions can be drawn as follows: decreasing the MTD of the evaporator (curve 5′-5-3 shifts left), which means a higher exhaust gas utilization efficiency, can decrease the internal and external exergy destruction of the evaporator; decreasing the condensing temperature (curve 3-3′-2 shifts down and point 2 shifts left to increase the expander output power) or increasing the isotropic efficiency of the expander (point 2 shifts toward point 2s to deduce the exergy destruction in the expander), which means a higher Rankine cycle efficiency, can decrease the exergy destruction of the condenser and increase the expander output power; increasing the evaporating temperature (curve 5-5′ shifts up and curve 3-5 shift right to keep the MTD constant) has a complex effect on the exergy destruction of the evaporator, so does increasing the superheating temperature (point 1 shifts up, point 5′ shifts left, and point 3 shifts right to keep the proportion of preheating, evaporating and superheating processes). Obviously effects of those parameters on the Rankine cycle performance from the viewpoints of energy balance and exergy balance agree well with each other.

3. Working fluid selection and system constraints

3.1. Working fluid selection

Working fluids of Rankine cycles can be classified according to the slope of the saturated vapor line in the *T–s* diagram into three types: wet, isentropic and dry fluids [29]. Fixing the heat source temperature at 600K, Wang et al. [11] indicated that R113, R123, R11 and R142b manifest slightly higher thermodynamic performances as organic Rankine cycle working fluids for engine WHR, and R245fa and R245ca are the most environment-friendly working fluids. Domingues et al. [30] revealed the advantage of using water as the working fluid in applications of thermal recovery from high temperature exhaust gas of a spark-ignition engine. In this part, both typical wet fluids (water, ethanol) and dry fluids (R113, R123 and R245fa) were compared to study the effects of working fluid properties on system performances with different heat source temperatures.

As shown in Fig. 5, the wet fluids have high critical temperatures and large latent heat compared with the dry fluids. To reduce the exergy destruction in the evaporator, temperature curves of the cold and hot sides should get close as shown in Fig. 4. So considering the critical temperature and the heat source temperature, it's better to choose wet fluids for high temperature waste heat sources and dry fluids for low temperature waste heat sources. Since the wet fluids have larger latent heat, the needed mass flow rate is relatively small. As the solid line shown in Fig. 3, the MTD always occurs at the pinch point of the evaporating process according to Eq. (5). For dry fluids with small latent heat, the needed mass flow rate is always large to achieve the same output power, which makes the MTD occur at the inlet point of the working fluid, just as the dash line shown in Fig. 3. So the *T–s* diagrams can provide a general assessment of working fluids for different waste heat sources of ICEs.

3.2. Constraints of WHR system

For different kinds of ICEs, principles of the Rankine cycle design are different in respect of system configurations, working fluids and operating parameters. Also the requirements for system components are more restricted considering the vehicle operation. The restricted conditions can be divided into two categories: thermodynamic constraints and component constraints, as shown in Fig. 6.

Thermodynamic constraints include heat source conditions, working fluid properties and condensation conditions. Since the exhaust gas temperature of the gasoline engine can be very high, BMW [3] and Honda [4] chose water as the working fluid due to its high critical temperature and large evaporating enthalpy. Working fluids with small latent heat are always selected in the diesel engine WHR system to insure the superheated state of the vapor out of the evaporator, such as ethanol chosen by AVL and Daimler [19,31] and R245fa chosen by Cummins and ORL [5,6]. The condensing temperature should be as low as possible if the required driving force for condensation heat transfer is satisfied for a given condenser structure [29]. Since exhaust gas states vary with load conditions, control strategies are much complex to achieve the maximum

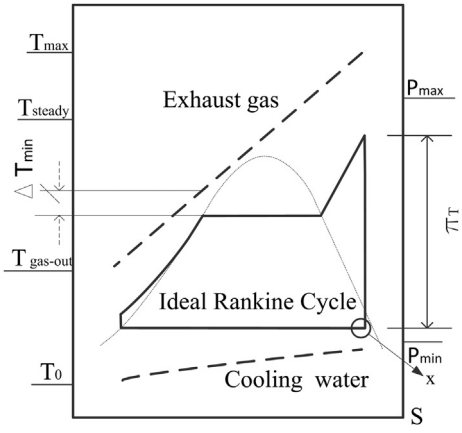

Fig. 6. Constraints of the system design.

utilization of waste heat, and that's why many manufacturers prefer to select heavy duty diesel engines or static engines whose working conditions are stable over a large portion of operating hours as research objects.

Component constraints include the type, size, installation and cost of every system component. As large components of the WHR system, the evaporator and condenser decide the needed space for installation. Since the gasoline engine is relatively small and the available space for system components is limited, compact heat exchangers become the first choice. While the diesel engine with high output has a bigger size and needs a larger working fluid mass flow rate, shell-tube heat exchangers are always used. Two kinds of expanders are always adopted: one is turbine expender, and the other is reciprocating expander. Wang et al. [32] indicated that the turbine expander is preferred to be applied when the waste heat recovered is converted into electrical energy, while the reciprocating expander is considered to be more appropriate for combining mechanical output directly to the crankshaft. Also the technology of the turbine expander is mature, and the isentropic efficiency and cost are higher. In addition, there are many other factors which need to be considered, such as the allowable temperature range of the exhaust gas in the evaporator, the dryness of the working fluid out of the expander, the pressure head and the volume flow rate range of the pump and the sequence of the evaporator and after treatment equipments.

Drawn from predecessors' research work, those two kinds of constraints are listed as follows and should be considered in the simulation and experimental researches.

1) The temperature range of the bottoming Rankine cycle is restricted by the heat source temperature T_{max} and the environment temperature T_0.
2) The minimum temperature difference ΔT_{min} in the evaporator and condenser should be larger than 10K to ensure the driving force of heat transfer processes [9].
3) The superheating temperature of the working fluid out of the evaporator should not exceed the maximum thermal steady temperature T_{steady}. Working fluids with strong hydrogen bonds usually are very steady at high temperature, and many organic fluids start to decompose at 650K [33].
4) The outlet temperature of the exhaust gas $T_{gas\ out}$ should be higher than 90 °C to protect the evaporator from fouling [34].
5) The minimum condensing pressure P_{min} should be larger than 1 bar in order to reduce the cost of system seal. The dryness x of the working fluid after expanding should be larger than 0.9 to eliminate the impingement of liquid droplets on the turbine blades [30].
6) The maximum evaporating pressure P_{max} should be lower than 35 bar, otherwise the cost of every component will rise quickly [15].
7) Different kinds of expenders can reach different expanding ratios π_t and isotropic efficiencies. For a single stage turbine, the expanding ratio is always no larger than 10 [33].
8) The evaporating temperature should be less than 0.85 times of the critical temperature since too large evaporating temperature will only increase the cost of the system and show few effects on the Rankine cycle efficiency [29].

4. Results and discussions

To investigate effects of the evaporating pressure and the superheating temperature on system performances which cannot be obtained from the theoretical analyses, thermodynamic models of the WHR system were built in Matlab software based on the analyses above, and working fluid properties were calculated with REFPROP [35], which was developed by the National Institute of Standards and Technology of the United States. Considering exhaust gas conditions and system design constraints of different types of ICEs, the values of primary system parameters were selected as follows: the exhaust gas temperature ranged from 550 to 1000K; the evaporating pressure ranged from 5 to 26 bar; the MTD of the evaporator was fixed at 30K; the condensing temperature was set at 330K, and the condensing pressure was kept larger than 1 bar at the same time; the outlet temperature of the exhaust gas were kept larger than 363K; firstly there was no superheating for dry fluids before the turbine, and the dryness of the vapor out of the turbine should be larger than 0.9 for wet fluids; the isentropic efficiencies of the turbine and the pump both were assumed to be 0.8.

4.1. Influences of heat source temperature and evaporating pressure

Fig. 7 shows influences of the evaporating pressure, heat source temperature and working fluid properties on the global recovery efficiency of the WHR system, and conclusions can be drawn as follows:

1. Ethanol and R113 show better thermodynamic performances in the whole operating regions; water becomes the best choice when the heat source temperature is higher than 800K. So without knowing the temperature range of waste heat, it is difficult to recommend the working fluid.
2. For all those working fluids, the contours of global recovery efficiencies are smooth when the heat source temperature is relatively low. That is because the Rankine cycle efficiency and the exhaust gas utilization efficiency change adversely with the increase of the evaporating pressure, which can be learned from Eq. (15) and Fig. 4. With high exhaust gas temperatures, the exhaust gas utilization efficiency changes slowly as shown in the first part of Eq. (15) or (16), and the effect of the Rankine cycle efficiency is dominant, which makes the global recovery efficiency increase dramatically with the increase of the evaporating pressure.
3. There exists an optimal evaporating pressure with water as the working fluid under low exhaust gas temperature conditions, which has been concluded in the discussion of Eq. (15). For other working fluids, there exists no optimal evaporating pressure because the temperature of exhaust gas is relative higher compared with their critical temperatures.
4. For those dry fluids with low critical temperatures and small latent heat, the exhaust gas temperature out of the evaporator, which determines the exhaust gas utilization efficiency, is restricted at 363K, and the global recovery efficiency is determined by Eq. (16) and mainly depends on the Rankine cycle efficiency.
5. Compared with R113 and R123, R245fa shows relatively poor thermodynamic performances but is the most environment-friendly working fluid, which makes it the best choice for the low-grade WHR system.
6. For all the working fluids, the efficiency curves become smooth when the evaporating pressure increases to a certain value. Therefore, the value of the evaporating pressure should not be too high from the cost-effective view.

4.2. Effects of superheating temperature

Assuming the heat source temperature was 750K, the evaporating pressure was 20 bar, and the superheating temperature, which was restricted by the maximum thermal steady temperature

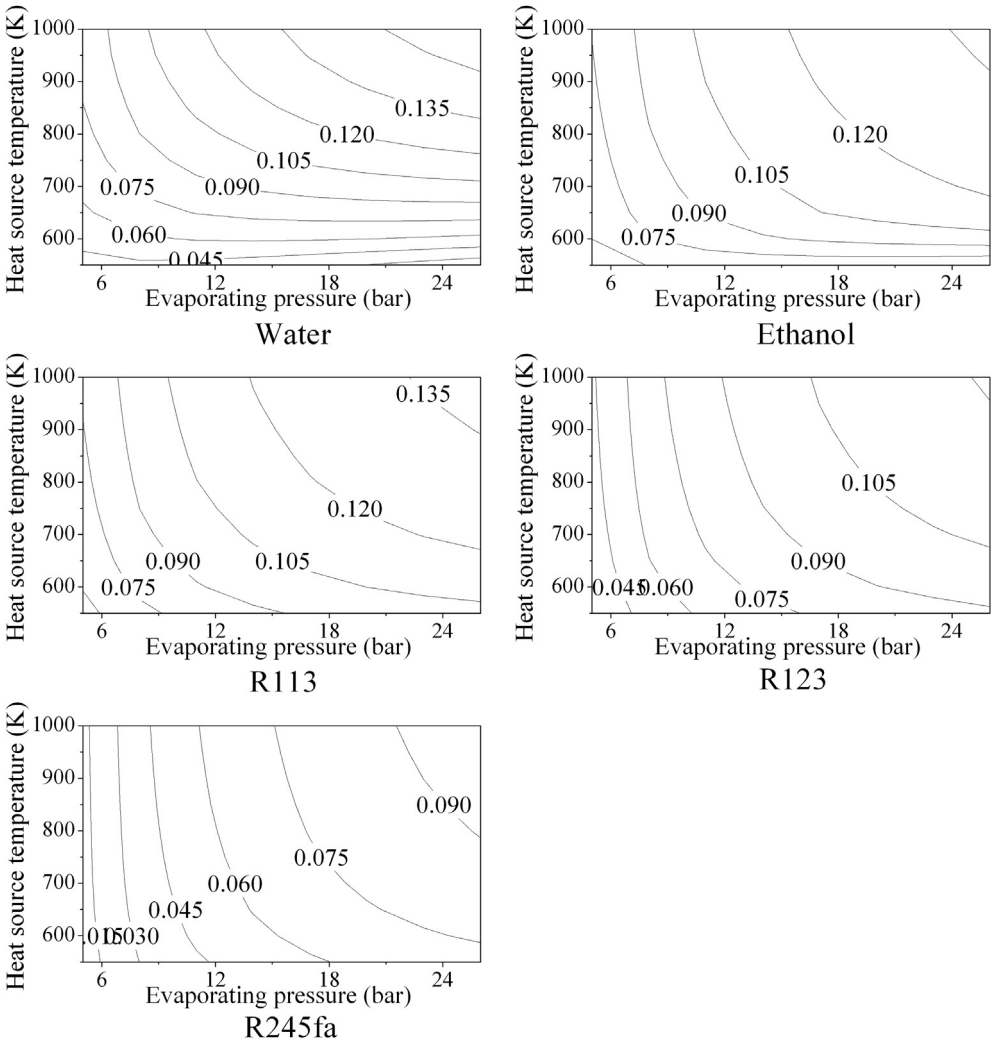

Fig. 7. Contour maps of global recovery efficiencies with different working fluids.

of organic fluids, ranged from 0 to 70K, Fig. 8 shows influences of the superheating temperature on the global recovery efficiencies with different working fluids, and the conclusions can be drawn as follows: superheating decreases the global recovery efficiencies for dry fluids and increases the global recovery efficiencies for wet fluids, which mainly depends on the working fluid properties [2]. Also the superheating temperature has a small effect on the global recovery efficiency, which can also be deduced from Eqs. (15) and (16).

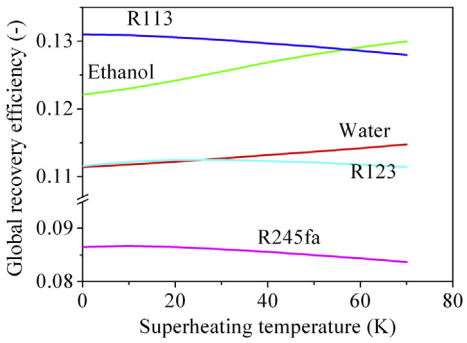

Fig. 8. Effects of superheating temperature on the global recovery efficiency.

Fig. 9 shows the relationship between the superheating temperature and the mass flow rate when unit mass flow rate of the exhaust gas is studied. It can be seen that water has the smallest mass flow rate followed by ethanol. Because of the small evaporating enthalpy, dry fluids need large mass flow rates which are almost ten or more times larger than that of water. With the increasing of the superheating temperature, mass flow rates of dry fluids drop dramatically, which in return reduces the cost and size of every system component, and that's why most dry fluids need to be superheated when vehicle installation is considered. If the superheating temperature is too large, a recuperator can be equipped to improve the recovery efficiency and release the load of the condenser but increase the complication and cost of the whole system at the same time. Since dry fluids always have high density, the volume flow rates are not so large compared with those of wet fluids. Ethanol has the largest volume flow rate among the five working fluids, which becomes the main shortcoming as the working fluid for the WHR system.

4.3. Effects on exergy distributions

Selecting water as the working fluid, Fig. 10 shows effects of the evaporating pressure on exergy distributions when the exhaust gas temperature was set at 750K. The exergy destruction rate in the

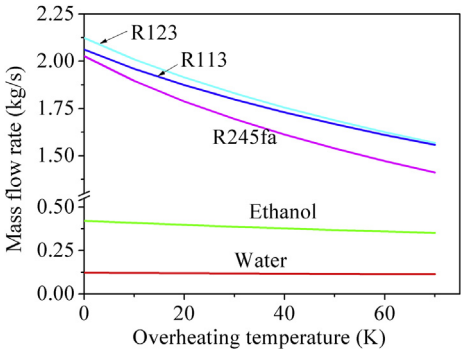

Fig. 9. Effects of superheating temperature on the mass flow rate.

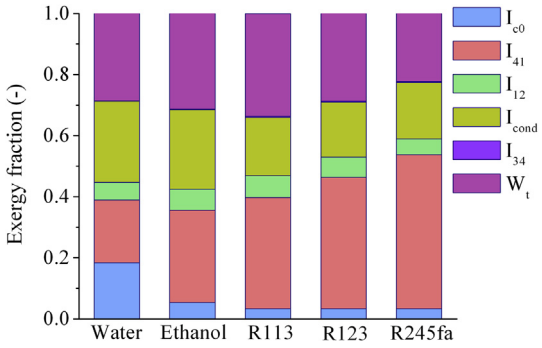

Fig. 11. Distributions of exergy destruction with different working fluids.

pump is invisible due to the small quantity. With the increase of the evaporating pressure, the temperature difference between hot and cold fluids decreases, which leads to a decrease of the internal exergy destruction of the evaporator. At the same time, the driving force is weakened and the heat flux in the evaporator reduces, which lead to a large outlet temperature of the exhaust gas and big external exergy destruction of the evaporator. Those two kinds of exergy destruction vary differently with the increase of the evaporating pressure and determine the total exergy destruction of the evaporator. A similar phenomenon can also be observed in Fig. 4. Since the exergy destruction in the turbine, condenser and pump remains almost the same, the output power of the turbine increases rapidly at first and then smoothly. The optimal evaporating pressure doesn't occur under the given operating condition, which is consistent with the results shown in Fig. 7. The exergy analyses indicate that the exergy destruction of the evaporator and condenser accounts for approximate 70% of the input exergy of the heat source.

Fig. 11 shows the distributions of exergy destruction with different working fluids when the exhaust gas temperature and the evaporating pressure are assumed to be 750K and 20 bar, respectively. The exergy destruction rate in the pump is also invisible due to the small quantity. It can be seen that ethanol and R113 have higher exergy efficiencies, and R245fa shows a relatively bad performance. For wet fluids, the condensing temperature is relatively high to insure the condensing pressure larger than 1 bar, which makes the exergy destruction of the condenser larger than that of dry fluids. With the same evaporating pressure, water has a high evaporating temperature, which makes the internal exergy destruction of the evaporator lower and the external exergy destruction higher. For dry fluids, the MTD in the evaporator is mainly restricted by the minimum allowable outlet temperature of the exhaust gas, which results higher internal exergy destruction and lower external exergy destruction. The exergy destruction in the pump of dry fluids is much higher than that of wet fluids, but it can still be neglected compared with the turbine output power.

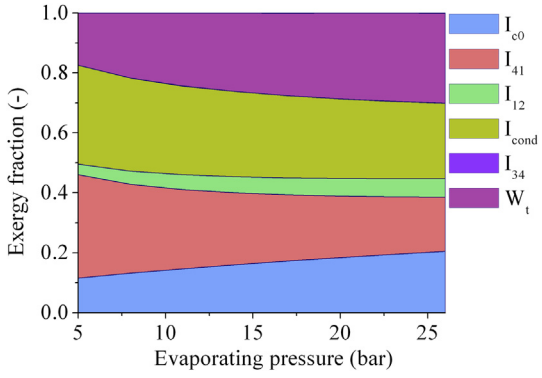

Fig. 10. Effects of evaporating pressure on exergy distributions.

5. Conclusions

In this paper, a theoretical formula was presented to investigate the influences of primary operating parameters on the Rankine cycle performance for engine WHR, and an exergy flow map was drawn for theoretical analyses of the exergy destruction processes. Five typical working fluids were compared with the thermodynamic models built in Matlab. The following are the conclusions.

1. The point at which the MTD of the evaporator occurs mainly depends on the mass flow rate and properties of the working fluid. For dry fluids, the MTD always occurs at the inlet of the working fluid in the evaporator when the exhaust gas temperature is relatively high.
2. The influences of the evaporating pressure and the superheating temperature on the global recovery efficiency are complicated and mainly depend on the working fluid properties. Superheating is essential for dry fluids to reduce the component size and for wet fluids to protect the turbine blades.
3. The global recovery efficiency is no larger than 0.14 under typical operating conditions. Ethanol and R113 show better performances in the whole exhaust temperature range.
4. With the increasing of the evaporating pressure, the internal exergy destruction of the evaporator decreases, and the external exergy destruction increases. Most working fluids do not have the optimal evaporating pressure due to the relatively high exhaust gas temperature.
5. For different kinds of working fluids and design constraints, the distributions of exergy destruction of system components are varied, which shows directions for improving different WHR systems.

Acknowledgments

This work was sponsored by the National Pre-Research Project (Project No. 62201020203) during the 12th Five-Year Plan Period.

References

[1] Saidur R, Rezaei M, Muzammil WK, Hassan MH, Paria SP, Hasanuzzaman M. Technologies to recover exhaust heat from internal combustion engines. Renewable and Sustainable Energy Reviews 2012;16:5649–59.
[2] Chen H, Goswami DY, Stefanakos EK. A review of thermodynamic cycles and working fluids for the conversion of low-grade heat. Renewable and Sustainable Energy Reviews 2010;14:3059–67.

[3] Ringler J, Seifert M, Guyotot V, Hübner W. Rankine cycle for waste heat recovery of IC engines. SAE technical paper 2009-01-0174.
[4] Endo T, Kawajiri S, Kojima Y, Takahashi K, Baba T, Ibaraki S, et al. Study on maximizing exergy in automotive engines. SAE technical paper 2007-01-0257.
[5] Nelson C. Exhaust energy recovery. In: Proceedings of directions in energy-efficiency and emissions research (DEER) conference. Dearborn, Michigan. Presentation available from: www1.eere.energy.gov/vehiclesandfuels/pdfs/deer_2008/session5/deer08_nelson.pdf; 2008 [last accessed 06.06.13].
[6] Briggs TE, Wagner R, Edwards KD, Curran S, Nafziger E. A waste heat recovery system for light duty diesel engines. SAE technical paper 2010-01-2205.
[7] Zhang X, Zeng K, Bai S, Zhang Y, He M. Exhaust recovery of vehicle gasoline engine based on organic Rankine cycle. SAE technical paper 2011-01-1339.
[8] Park T, Teng H, Hunter GL, Velde BVD, Klaver J. A Rankine cycle system for recovering waste heat from HD diesel engines – experimental results. SAE technical paper 2011-01-1337.
[9] Serrano JR, Dolz V, Novella R, García AHD. Diesel engine equipped with a bottoming Rankine cycle as a waste heat recovery system. Part 2: evaluation of alternative solutions. Applied Thermal Engineering 2012;36:279–87.
[10] Vaja I, Gambarotta A. Internal combustion engine (ICE) bottoming with organic Rankine cycles (ORCs). Energy 2010;35:1084–93.
[11] Wang EH, Zhang HG, Fan BY, Ouyang MG, Zhao Y, Mu QH. Study of working fluid selection of organic Rankine cycle (ORC) for engine waste heat recovery. Energy 2011;36:3406–18.
[12] Katsanos CO, Hountalas DT, Pariotis EG. Thermodynamic analysis of a Rankine cycle applied on a diesel truck engine using steam and organic medium. Energy Conversion and Management 2012;60:68–76.
[13] Arias DA, Shedd TA, Jester RK. Theoretical analysis of waste heat recovery from an internal combustion engine in a hybrid vehicle. SAE technical paper 2006-01-1605.
[14] Srinivasan KK, Mago PJ, Krishnan SR. Analysis of exhaust waste heat recovery from a dual fuel low temperature combustion engine using an Organic Rankine Cycle. Energy 2010;35:2387–99.
[15] Chammas RE, Clodic D. Combined cycle for hybrid vehicles. SAE technical paper 2005-01-1171.
[16] Shu G, Zhao J, Tian H, Liang X, Wei H. Parametric and exergetic analysis of waste heat recovery system based on thermoelectric generator and organic Rankine cycle utilizing R123. Energy 2012;45:806–16.
[17] Yu G, Shu G, Tian H, Wei H, Liu L. Simulation and thermodynamic analysis of a bottoming Organic Rankine Cycle (ORC) of diesel engine (DE). Energy 2013;51:281–90.
[18] Tian H, Shu G, Wei H, Liang X, Liu L. Fluids and parameters optimization for the organic Rankine cycles (ORCs) used in exhaust heat recovery of Internal Combustion Engine (ICE). Energy 2012;47:125–36.
[19] Teng H. Waste heat recovery concept to reduce fuel consumption and heat rejection from a diesel engine. SAE technical paper 2010-01-1928.
[20] Wang D, Ling X, Peng H, Liu L, Tao L. Efficiency and optimal performance evaluation of organic Rankine cycle for low grade waste heat power generation. Energy 2013;50:343–452.
[21] Wang J, Yan Z, Wang M, Ma S, Dai Y. Thermodynamic analysis and optimization of an (organic Rankine cycle) ORC using low grade heat source. Energy 2013;49:356–65.
[22] He C, Liu C, Gao H, Xie H, Li Y, Wu S, et al. The optimal evaporation temperature and working fluids for subcritical organic Rankine cycle. Energy 2012;38:136–43.
[23] Rakopoulos CD, Giakoumis EG. Second-law analyses applied to internal combustion engines operation. Progress in Energy and Combustion Science 2006;32:2–47.
[24] Rakopoulos CD, Kyritsis DC. Comparative second-law analysis of internal combustion engine operation for methane, methanol, and dodecane fuels. Energy 2001;26:705–22.
[25] Rakopoulos CD, Scott MA, Kyritsis DC, Giakoumis EG. Availability analysis of hydrogen/natural gas blends combustion in internal combustion engines. Energy 2008;33:248–55.
[26] Rakopoulos CD, Michos CN, Giakoumis EG. Availability analysis of a syngas fueled spark ignition engine using a multi-zone combustion model. Energy 2008;33:1378–98.
[27] Moran MJ. Availability analysis: a guide to efficient energy use. New Jersey, USA: Prentice-Hall, Englewood Cliffs; 1982.
[28] Zhu MS. The exergy analysis of waste heat recovery system for power. Journal of Engineering Thermophysics 1982;3(2):113–9 [in Chinese].
[29] Teng H, Regner G, Cowland C. Waste heat recovery of heavy-duty diesel engines by organic Rankine cycle part II: working fluids for WHR-ORC. SAE technical paper 2007-01-0543.
[30] Domingues A, Santos H, Costa M. Analysis of vehicle exhaust waste heat recovery potential using a Rankine cycle. Energy 2013;49:71–85.
[31] Rakesh A, Sandeep S, Kevin S. Exhaust heat driven Rankine cycle for a heavy duty diesel engine. In: 2011 DEER conference. Detroit. Presentation available from: www1.eere.energy.gov/vehiclesandfuels/pdfs/deer_2011/wednesday/presentations/deer11_singh.pdf; 2011 [last accessed 06.06.13].
[32] Wang T, Zhang Y, Peng Z, Shu G. A review of researches on thermal exhaust heat recovery with Rankine cycle. Renewable and Sustainable Energy Reviews 2011;15:2862–71.
[33] Latz G, Andersson S, Munch K. Comparison of working fluids in both subcritical and supercritical Rankine cycles for waste-heat recovery systems in heavy-duty vehicles. SAE technical paper 2012-01-1200.
[34] Li Y-R, Wang J-N, Du M-T. Influence of coupled pinch point temperature difference and evaporation temperature on performance of organic Rankine cycle. Energy 2012;42:503–9.
[35] REFPROP version 7.1, NIST standard reference database 23. America: The US Secretary of Commerce; 2003.